Acta Crystallographica Section D
Biological Crystallography
ISSN 0907-4449

Crystallization and preliminary crystallographic analysis of yeast cytosine deaminase

Yi-Hsin Hsu,[a]† Chih-Yung Hu,[b]† Jing-Jer Lin[a] and Shwu-Huey Liaw[b,c,d]*

[a]Institute of Biopharmaceutical Science, National Yang-Ming University, Taipei, Taiwan, [b]Institute of Biochemistry, National Yang-Ming University, Taipei, Taiwan, [c]Department of Life Science, National Yang-Ming University, Taipei, Taiwan, and [d]Department of Medical Research and Education, Taipei Veterans General Hospital, Taipei, Taiwan

† These authors contributed equally to the work.

Correspondence e-mail: shliaw@ym.edu.tw

Received 22 January 2002
Accepted 13 March 2003

Cytosine deaminase is an attractive candidate for anticancer gene therapy through its catalysis of the deamination of the prodrug 5-fluorocytosine to 5-fluorouracil. Recombinant yeast cytosine deaminase has been crystallized with the inhibitor 2-hydroxypyrimidine in 10% 2-propanol, 20% polyethylene glycol 4000, 0.1 *M* HEPES pH 7.5. The crystals belong to space group $P2_1$, with unit-cell parameters $a = 45.31$, $b = 53.33$, $c = 64.29$ Å, $\beta = 99.98^\circ$ and one dimer per asymmetric unit. The crystals diffract X-rays beyond 1.5 Å resolution and an initial atomic model has been built based on selenomethionyl multiwavelength anomalous data at 2 Å resolution.

1. Introduction

Cytosine deaminase (EC 3.5.4.1) catalyzes the deamination of cytosine to uracil and 5-methylcytosine to thymine. The enzyme has been found in bacteria and fungi, where it plays an important role in pyrimidine salvage. However, it is not present in mammalian cells, which instead utilize cytidine deaminases (Nishiyama *et al.*, 1985). The bacterial and fungal cytosine deaminases are distinct and have evolved separately: the 426-residue hexameric *Escherichia coli* enzyme belongs to the $(\beta/\alpha)_8$-barrel amidohydrolase superfamily (Ireton *et al.*, 2002; Liaw *et al.*, 2003), while the 158-residue dimeric yeast counterpart does not display any sequence homology to the bacterial enzymes (Erbs *et al.*, 1997).

The antimetabolite 5-fluorouracil (5-FU) is one of the most active chemotherapeutic agents for the treatment of colorectal cancer, but has limited efficacy owing to its gastrointestinal and haematological toxicity (Vauthey *et al.*, 1996). Owing to its ability to convert the relatively non-toxic 5-fluorocytosine (5-FC) into 5-FU and its absence in mammalian cells, cytosine deaminase becomes an attractive candidate for enzyme-prodrug gene therapy because of its ability to reduce the toxicity of 5-FU toward normal distal tissues (Greco & Dachs, 2001). Currently, a combination of 5-FC with cytosine deaminases has proved effective in controlling tumour growth in animals and is being evaluated in several human clinical trials (Miller *et al.*, 2002; Nyati *et al.*, 2002). Previous studies have also suggested that the single tested yeast cytosine deaminase is a better candidate for gene therapy, perhaps owing to the yeast enzyme's higher efficiency of conversion of 5-FC into 5-FU (Kievit *et al.*, 1999, 2000). To provide structural insights into the catalytic mechanism, evolution and gene-therapy applications of the yeast cytosine deaminase, we have obtained protein crystals and have solved the phase problem using the selenomethionyl multiwavelength anomalous dispersion method.

2. Protein preparation, crystallization and X-ray data analysis

The 158-residue *Saccharomyces cerevisiae* cytosine deaminase was expressed using the vector pET-6H (a gift from Dr C. H. Hu at the National Marine University, Taiwan) in *E. coli* BL21 pLysS and in *E. coli* B834 (DE3) for the selenomethionyl labelled protein. The recombinant protein contains eight additional vector residues at the N-terminus including a six-His tag. 1 l cultures were grown at 298 K to an OD_{600} of 0.5 and were induced by the addition of 1 m*M* isopropyl-β-D-thiogalactopyranoside (IPTG). The cells were grown at 298 K for another 4 h prior to harvest. The cells were resuspended in 10 ml of buffer containing 50 m*M* NaH_2PO_4 pH 7.8, 300 m*M* NaCl, 10 m*M* imidazole and protease inhibitors (Calbiochem) and were lysed by sonication. After removal of cellular debris by centrifugation at 13 000*g* at 277 K for 15 min, 0.5 ml Ni–NTA resin (Qiagen) was added to the supernatant and incubated at 277 K for 1 h. The resin was washed and the protein was eluted with 2 ml of buffer containing 50 m*M* NaH_2PO_4 pH 8.0, 300 m*M* NaCl and 250 m*M* imidazole. To purify the selenomethionyl labelled protein, the cells were incubated overnight at 310 K in LB medium containing 100 µg ml^{-1} ampicillin and then inoculated into 7 l LeMaster medium supplemented with

50 mg l^{-1} seleno-DL-methionine (Hendrickson *et al.*, 1990). After IPTG induction, the cells were grown for another 16 h at 298 K. The selenomethionyl protein was purified in a similar way to the native protein.

Initial crystallization screening was performed with Hampton Crystal Screens using the hanging-drop vapour-diffusion method at 295 and 277 K. The crystals were grown in 10% 2-propanol, 20% polyethylene glycol 4000 and 0.1 *M* Na HEPES pH 7.5, with a combination of 2 µl reservoir solution and 2 µl protein solution (30 mg ml^{-1}) in the presence of various amounts (0–20 m*M*) of the transition-state analogue 2-hydroxypyrimidine (Aldrich). Crystals appeared after 3–5 d and reached their final dimensions in 1–2 weeks at 295 K (Fig. 1). A seeding experiment was employed to enlarge the crystal size and reduce the crystallization time to 2–3 d. The selenomethionyl protein was crystallized under the same conditions.

X-ray diffraction data were collected at 100 K with the addition of 5% glycerol as a cryoprotectant. The crystals diffract to 2.5 Å resolution using in-house radiation, but diffract to beyond 1.5 Å resolution using synchrotron radiation. Data were collected using an ADSC Quantum 4 CCD camera at beamlines BL-6A and BL-18B at the Photon Factory and beamlines BL12B and BL41XU at SPring-8. Data were processed using the program *HKL* (Otwinowski & Minor, 1997). The phase problem was solved by multiwavelength anomalous diffraction using selenomethionines as the anomalous diffractor using *SOLVE*; initial dimeric models were built by *RESOLVE* (Terwilliger & Berendzen, 1999).

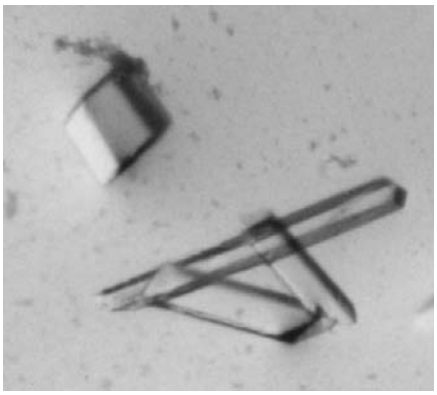

Figure 1
Yeast cytosine deaminase crystals. Two crystal morphologies were commonly observed: prismatic crystals with typical dimensions of 0.2 × 0.2 × 0.15 mm and long thin rod-shaped crystals with dimensions of 0.5 × 0.1 × 0.05 mm. The rod crystals appeared more often, but diffracted X-rays poorly.

Table 1
Statistics for native and selenium multiwavelength anomalous data collection.

Values in parentheses are for the highest resolution shell.

	Se peak	Se inflection	Se remote	Native
Wavelength (Å)	0.9793	0.9795	0.9717	0.71
Resolution (Å)	50–2.0 (2.03–2.0)	50–2.0 (2.03–2.0)	50–2.0 (2.03–2.0)	50–1.6 (1.63–1.6)
Observed reflections	75997	76810	75274	176022
Unique reflections	16223	16284	16258	38939
Completeness (%)	79.0 (45.4)	79.1 (45.6)	79.1 (45.5)	90.1 (90.9)
Averaged $I/\sigma(I)$	16.9	17.7	19.7	11.9
$R_{\rm merge}$ (%)	8.6 (16.8)	7.2 (15.5)	7.5 (17.5)	4.9 (24.4)
Overall figure of merit		0.49		

3. Results and discussion

To date, the recombinant enzyme could not be crystallized in the absence of inhibitors. The selenomethionyl protein required an even higher concentration of inhibitors. Autoindexing and consideration of systematically absent reflections revealed the crystals to belong to the space group $P2_1$. Crystals grown at varying inhibitor concentrations have slightly different unit-cell parameters. For example, selenomethionyl crystals grown in 15 m*M* 2-hydroxypyrimidine had unit-cell parameters $a = 45.31$, $b = 53.33$, $c = 64.29$ Å, $\beta = 99.98^\circ$, while the parameters of the native crystals with 2 m*M* 2-hydroxypyrimidine were $a = 47.11$, $b = 53.68$, $c = 68.08$ Å, $\beta = 105.33^\circ$. Changes in the unit-cell parameters as the concentration of inhibitor increases suggest that there may be conformational changes in the enzyme structure on binding of substrate or inhibitor. The packing density suggests that there is one dimer per asymmetric unit ($V_{\rm M} = 2.4$ Å^3 Da^{-1}), with a solvent content of 48%. Both native and selenomethionyl multiple anomalous data have been collected; the data statistics are summarized in Table 1.

Ten Se positions were identified with *SOLVE* based on the selenomethionyl anomalous data; an initial dimeric model with 168 polyalanine residues in 19 chains was then built by *RESOLVE*, revealing a similar structural core to that of cytidine deaminase, made up of one long helix (αA) and a five-stranded β-sheet (β1–β5). The partial model was then compared with cytidine deaminases from *Bacillus subtilis* (PDB code 1jtk; Johansson *et al.*, 2002) and from *E. coli* (PDB code 1aln; Betts *et al.*, 1994), revealing a possible structural homology despite the lack of sequence similarity. The cytidine deaminase structures were used to assist in sequential assignment of the 19 chains in the model, in addition to the Se peaks (Fig. 2). For example, chain 2 with residues 202–220 near to the Se-7 peak and

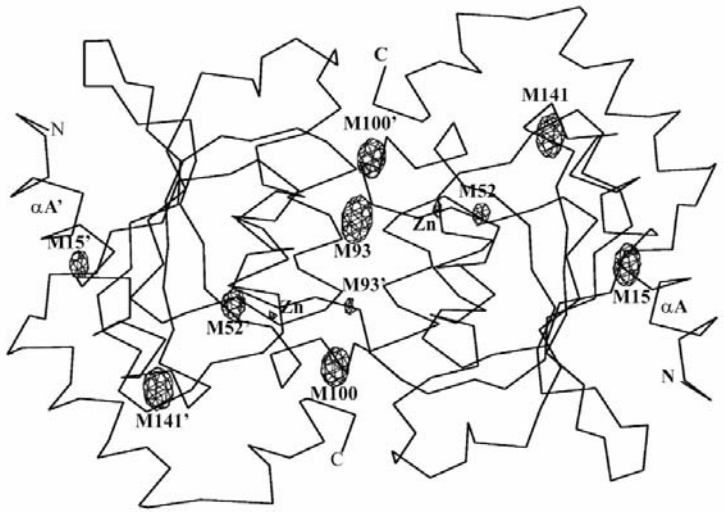

Figure 2
The C^α trace of dimeric yeast cytosine deaminase, with the Se anomalous difference Fourier map contoured at 10σ showing the ten selenium and two zinc peaks. The enzyme contains seven methionines per subunit; Met1 and Met6 were disordered and only the Se peaks of Met15, Met52, Met93, Met100 and Met141 were observed. Met93 is so close to Met100′ of the adjacent subunit that the Se peak of Met93 was incorrectly grouped with that of Met100′ during the initial NCS search with *RESOLVE*.

chain 4 with residues 402–418 near to the Se-9 peak were assigned as the N-terminal long helix (αA) containing Met15; chains 12 (1202–1209) and 15 (1502–1508) were assigned as strand β1, followed by β2, αB, β3, αC, β4 and β5. The assignment suggested three β-strands (β1, β2 and β5) were modelled in the opposite direction, N-terminus to C-terminus instead of C-terminus to N-terminus. In addition, Met93 appears closer to Met100′ of the adjacent subunit than to Met100 (Fig. 2). The short distance between Met93 and Met100′ led to the incorrect grouping of their Se peaks, resulting in incorrect non-crystallographic symmetry axes (NCS) for the search using *RESOLVE*. A more complete dimeric model with 218 poly-alanine residues was generated by *RESOLVE* after a correct NCS analysis and the overall NCS correlation increased from 0.56 to 0.78.

Based on the Fourier electron-density map generated by the selenomethionyl data, 52 further residues, mostly side chains, the inhibitor 2-hydroxypyrimidine and two zinc ions were introduced into the model. Further structural refinement based on a higher resolution data set is still in progress. This should provide new information on the enzyme with respect to substrate specificity, its evolution and its potential gene-therapy applications.

The synchrotron-radiation experiments were performed at the Synchrotron Radiation Research Center, Taiwan, at the Photon Factory (Proposal No. 2002G309), Japan and at SPring-8 with the approval of the Japan Synchrotron Radiation Research Institute (Proposal No. 2003A0004-NL1-np). This study was partly supported by VGH 91-376-6, National Science Council Grant NSC 91-3112-B-010-012 to S-HL and by grant 89-B-FA22-2-4 (Program for Promoting Academic Excellence of Universities) to J-JL.

References

Betts, L., Xiang, S., Short, S. A., Wolfenden, R. & Carter, C. W. (1994). *J. Mol. Biol.* **235**, 635–656.
Erbs, P., Exinger, F. & Jund, R. (1997). *Curr. Genet.* **31**, 1–6.
Greco, O. & Dachs, G. U. (2001). *J. Cell. Physiol.* **187**, 22–36.
Hendrickson, W. A., Horton, J. & LeMaster, D. M. (1990). *EMBO J.* **9**, 1665–1672.
Ireton, G. C., McDermott, G., Black, M. E. & Stoddard, B. L. (2002). *J. Mol. Biol.* **315**, 687–697.
Johansson, E., Mejlhede, N., Neuhard, J. & Larsen, S. (2002). *Biochemistry*, **41**, 2563–2570.
Kievit, E., Bershad, E., Ng, E., Sethna, P., Dev, I., Lawrence, T. S. & Rehemtulla, A. (1999). *Cancer Res.* **59**, 1417–1421.
Kievit, E., Nyati, M. K., Ng, E., Stegman, L. D., Parsels, J., Ross, B. D., Rehemtulla, A. & Lawrence, T. S. (2000). *Cancer Res.* **60**, 6649–6655.
Liaw, S. H., Chen, S. J., Ko, T. P., Hsu, C. S., Chen, C. J., Wang, A. H. J. & Tsai, Y. C. (2003). *J. Biol. Chem.* **278**, 4957–4962.
Miller, C. R., Williams, C. R., Buchsbaum, D. J. & Gillespie, G. Y. (2002). *Cancer Res.* **62**, 773–780.
Nishiyama, T., Kawamura, Y., Kawamoto, K., Matsumura, H., Yamamoto, N., Ito, T., Ohyama, A., Katsuragi, T. & Sakai, T. (1985). *Cancer Res.* **45**, 1753–1761.
Nyati, M. K., Symon, Z., Kievit, E., Dornfeld, K. J., Rynkiewicz, S. D., Ross, B. D., Rehemtulla, A. & Lawrence, T. S. (2002). *Gene Ther.* **9**, 844–849.
Otwinowski, Z. & Minor, W. (1997). *Methods Enzymol.* **276**, 307–326.
Terwilliger, T. C. & Berendzen, J. (1999). *Acta Cryst.* D**55**, 849–861.
Vauthey, J. N., Marsh Rde, W., Cendan, J. C., Chu, N. M. & Copeland, E. M. (1996). *Br. J. Surg.*, **83**, 447–455.